Heliyon 10 (2024) e38250

Contents lists available at ScienceDirect

Heliyon

journal homepage: www.cell.com/heliyon

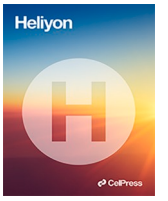

Research article

Deciphering miRNA signatures in axial spondyloarthritis: The link between miRNA-1-3p and pro-inflammatory cytokines

Aneta Prokopcova [a,b], Jiri Baloun [a], Kristyna Bubova [a,b,**], Monika Gregova [a], Sarka Forejtova [a,b], Jana Horinkova [a,b], Marketa Husakova [a,b], Katerina Mintalova [a], Vladimir Cervenak [c], Michal Tomcik [a,b], Jiri Vencovsky [a,b], Karel Pavelka [a,b], Ladislav Senolt [a,b,*]

[a] *Institute of Rheumatology, Na Slupi 450/4, 128 00, Prague, Czech Republic*
[b] *Department of Rheumatology, 1st Faculty of Medicine, Charles University, Katerinska 1660/32, 121 08, Prague, Czech Republic*
[c] *Department of Medical Imaging, St Anne's University Hospital and Faculty of Medicine, Masaryk University, Pekarska 664/53, 602 00, Brno, Czech Republic*

A R T I C L E I N F O

Keywords:
miRNA
Axial spondyloarthritis
Biomarkers
Cytokines
Profiling

A B S T R A C T

Axial spondyloarthritis (axSpA) is a chronic inflammatory disease that affects the spine and sacroiliac joints. Early detection of axSpA is crucial to slow disease progression and maintain remission or low disease activity. However, current biomarkers are insufficient for diagnosing axSpA or distinguishing between its radiographic (r-axSpA) and non-radiographic (nr-axSpA) subsets. To address this, we conducted a study using miRNA profiling with massive parallel sequencing (MPS) and SmartChip qRT-PCR validation. The goal was to identify differentially expressed miRNAs in axSpA patients, specifically those subdiagnosed with nr-axSpA or r-axSpA. Disease activity was measured using C-reactive protein (CRP) and the Ankylosing Spondylitis Disease Activity Score (ASDAS). Radiographic assessments of the cervical and lumbar spine were performed at baseline and after two years. Out of the initial 432 miRNAs, 90 met the selection criteria, and 45 were validated out of which miR-1-3p was upregulated, whereas miR-1248 and miR-1246 were downregulated in axSpA patients. The expression of miR-1-3p correlated with interleukin (IL)-17 and tumour necrosis factor (TNF) levels, indicating its significant role in axSpA pathogenesis. Although specific miRNAs distinguishing disease subtypes or correlating with disease activity or spinal changes were not found, the study identified three dysregulated miRNAs in axSpA patients, with miR-1-3p linked to IL-17 and TNF, underscoring its pathogenetic significance. These findings could help improve the early detection and treatment of axSpA.

1. Introduction

Axial spondyloarthritis (axSpA) is a relatively common chronic rheumatic disease characterised by inflammation of the sacroiliac joints (SIJ) and the spine, often accompanied by several extra-articular manifestations, including acute anterior uveitis, psoriasis, and inflammatory bowel disease. In 2009, the Assessment of Spondyloarthritis International Society (ASAS) validated the classification

* Corresponding author. Institute of Rheumatology, Na Slupi 450/4, 128 00, Prague, Czech Republic.
** Corresponding author. Institute of Rheumatology, Na Slupi 450/4, 128 00, Prague, Czech Republic.
E-mail addresses: bubova@revma.cz (K. Bubova), senolt@revma.cz (L. Senolt).

https://doi.org/10.1016/j.heliyon.2024.e38250
Received 13 April 2024; Received in revised form 12 September 2024; Accepted 20 September 2024
Available online 21 September 2024

criteria for axSpA, which included the definition of radiographic and non-radiographic subtypes [1]. The radiographic (r-axSpA) subtype, also known as ankylosing spondylitis (AS), is characterised as the advanced stage of the disease defined by bone erosion and new bone formation, which can gradually lead to ankylosis of the affected joints. However, these chronic inflammatory changes do not typically appear on radiographs at an early stage, which often results in a delayed diagnosis. The early stage of the disease, characterised by the absence of definite radiographically-defined sacroiliitis (minimally stage 3 unilaterally or stage 2 bilaterally) but with active inflammatory changes such as bone marrow edema visible on magnetic resonance imaging (MRI) of SIJs, is referred to as non-radiographic axSpA (nr-axSpA) [2]. Various studies have focused on the aetiology of nr-axSpA and have described the disease as heterogeneous, with an equal or even slight female predominance, lower rates of HLA-B27 positivity and less inflammatory activity based on CRP (C-Reactive Protein) and MRI when compared to r-axSpA [3,4]. Although only 10–20 % of nr-axSpA patients may progress to r-axSpA within two years after the disease onset [5], early diagnosis remains crucial for preserving the quality of life, identifying patients at higher risk of disease progression, and effectively managing inflammation and extra-articular manifestations.

Diagnosing axSpA based solely on MRI findings can sometimes result in misdiagnosis. Therefore, the current diagnostic approach relies on a combination of both imaging and clinical examination. It is worth noting that CRP levels have been found to be associated with disease progression, showing a significant increase (3.6-fold) in affected individuals [6]. Furthermore, there are several other inflammatory markers, including interleukin (IL)-6, IL-17, IL-23, and tumour necrosis factor (TNF), that have been found to have elevated blood levels in axSpA patients [7].

However, identifying nr-axSpA patients remains challenging despite advancements in disease understanding and methodological developments. MRI findings and biomarkers, such as HLA-B27, may be inconclusive, highlighting the need for the identification of new biomarkers. MicroRNAs (miRNAs) are considered potential biomarkers of various diseases, including rheumatoid arthritis (RA) or other rheumatic or musculoskeletal diseases [8,9]. MiRNAs are small non-coding RNAs that regulate up to 60 % of human mRNAs by either triggering the degradation of mRNAs or inhibiting protein translation [10]. They play a significant role in various biochemical and cellular processes and have been implicated in the pathogenesis of numerous diseases, including axSpA [11]. The expressions of miRNAs undergo dynamic changes during both physiological and pathological processes, as well as in response to treatments. Moreover, miRNAs can be detected in various sources, including blood, tissues, and body fluids. Their diagnostic precision has been utilised in various conditions, including osteoporosis, cardiovascular diseases, or thyroid cancer [8]. To date, several miRNAs (e.g. miR-17-5p, mir-27a, mir-29a, miR-130a) have been reported to be dysregulated in peripheral blood mononuclear cells (PBMCs) of axSpA patients [11,12]. It is important to note that miRNA research can often be technically heterogeneous, and the level of miRNAs can be influenced by various confounding factors, including age, sex, BMI (Body Mass Index), and circadian cycle [13].

This study aimed to discover miRNA biomarkers identifying patients with axSpA and distinguished the non-radiographic subset from radiographic, respectively. Additionally, we evaluated the ability of candidate miRNAs to monitor disease activity and predict progression in the spine over two years.

2. Materials and methods

2.1. Study population

This study included a total of 167 adult patients who were selected based on the ASAS classification criteria for axSpA [14]. The recruitment of participants for this study was conducted from 2014 to 2019 at the specialized early-spondyloarthritis office of the Institute of Rheumatology in Prague, involving three different clinicians. In order to ensure a representative sample, patients were selected with an emphasis on achieving a balanced distribution across gender and age demographics. The clinical characteristics of the participants are provided in Table 1. HCs were sourced from the biobank of the Institute of Rheumatology (Prague, Czechia) and had no history of musculoskeletal, inflammatory, autoimmune disease, or cancer. Written informed consent (ID: 7117/2018) was obtained from all subjects upon their enrolment in this study.

The study included a total of 85 patients with r-axSpA patients, 82 patients with nr-axSpA, and 72 HC. The screening cohort consisted of 96 individuals, including 38 with nr-axSpA, 38 with r-axSpA, and 20 healthy controls (HC). Validation analysis was conducted on 143 individuals, comprising 44 with nr-axSpA, 47 with r-axSpA, and 52 HC, including those patients with significant two-year radiographic progression ($n = 14$). Plasma samples from 80 individuals, including 27 with nr-axSpA, 27 with r-axspA, and 26 HC, were collected to determine cytokine levels.

Experienced rheumatologists conducted the clinical assessment using standardised methodologies, which included modified Schober test, occiput-to-wall and chin-to-chest distance, chest expansion, assessment of swollen joint count and tender joint count (SJC and TJC), physician global assessment (MDGAS), ASDAS, Bath Ankylosing Spondylitis Disease Activity Index (BASDAI), and Bath Ankylosing Spondylitis Functional Index (BASFI) [15,16]. ASDAS and BASDAI were categorised based on clinical recommendations [15]. CRP levels and erythrocyte sedimentation rate (ESR) were determined from blood samples collected on the same day as PBMCs sampling and clinical assessment. Additional diagnostic data were obtained at baseline (see Table 1).

X-Ray imaging was scheduled within a maximum of one week following both the blood sampling and clinical assessment. An experienced rheumatologist and a central radiologist independently assessed anonymised images for the initial disease classification. Any inter-observer discrepancies were resolved through a secondary evaluation until a consensus was reached. Patients who met the New York classification criteria [17] were classified as r-axSpA, while patients with sacroiliitis graded as less than two bilaterally or grade three unilaterally, along with positive MRI findings [such as characteristic bone marrow edema (BME)] were classified as nr-axSpA. The modified Stoke Ankylosing Spondylitis (mSASSS) was calculated for all sets of radiographs, and ΔmSASSS represented the difference between mSASSS at baseline and after two years. Radiographic progression was determined as ΔmSASSS $\geq$2. MRI of the

Table 1

Demographic and clinical characteristics of patients with nr-axSpA, r-axSpA, and control subjects in the screening and validation cohorts. axSpA represents the sum of the subgroups of nr-axSpA and r-axSpA All data are presented as median (IQR) unless otherwise specified. Abbreviations: ASDAS, Ankylosing Spondylitis Disease Activity Score; ASQoL, Ankylosing Spondylitis Quality of Life; axSpA, Axial Spondyloarthritis; BASDAI, Bath Ankylosing Spondylitis Disease Activity Index; BASFI, Bath Ankylosing Spondylitis Functional Index; bDMARDs, Biological Disease-Modifying Anti-Rheumatic Drugs; BMI, Body Mass Index; csDMARDs, Conventional Disease-Modifying Anti-Rheumatic Drugs; CRP, C-Reactive Protein; DA, Disease Activity; ESR, Erythrocyte Sedimentation Rate; EuroQol, European Quality of Life; MDGAS, Medical Doctor Global Assessment; mSASSS, Modified Stoke Ankylosing Spondylitis Spinal Score; Nr-Axspa, Non-Radiographic AxSpA; NSAIDs, Non-Steroidal Anti-Inflammatory Drugs; R-Axspa, Radiographic AxSpA; Scr, Screening; SJC, Swollen Joint Count; TJC, Tender Joint Count; Val, Validation.

Characteristics	HC (n = 72)		nr-axSpA (n = 82)		r-axSpA (n = 85)		axSpA (n = 169)		p-value	
	Scr (n = 20)	Val (n = 52)	Scr (n = 38)	Val (n = 44)	Scr (n = 38)	Val (n = 47)	Scr (n = 78)	Val (n = 91)	Scr	Val
Female, n (%)	9 (45)	26 (52.0)	22 (57.9)	24 (54.5)	10 (26.3)	16 (34.0)	32 (42.1)	40 (44.0)	**0.021**	*0.097*
Age [years]	36.5 (29.2–43.4)	40.1 (30.8–46.5)	39.9 (31.5–47.6)	38.7 (31.7–48.1)	36.9 (29.9–45.1)	37.5 (31.9–44.4)	37.9 (30.3–47.0)	38.3 (31.6–46.6)	0.667	0.913
Time since first symptom [years]	–	–	10 (2.69–14.44)	7.18 (2.01–18.43)	10.2 (2.97–14.97)	9.3 (4.02–13.90)	10.1 (2.94–14.92)	8.6 (2.73–14.75)	0.967	0.352
Time since diagnosis [years]	–	–	0.2 (0–0.62)	0.1 (0–0.75)	0.7 (0.14–3.70)	0.4 (0.04–2.81)	0.4 (0.01–2.43)	0.2 (0.01–2.16)	*0.074*	0.883
BMI [kg/m^2]	27.5 (22.3–28.8)	–	24.7 (21.6–27.4)	25.4 (23.2–28.4)	23.9 (22.4–26.7)	26.9 (23.2–29.2)	24.6 (21.9–27.6)	25.9 (23.2–29.1)	0.445	0.466
Smoker, n (%)	–	–	15 (39.5)	15 (35.7)	19 (50)	19 (45.2)	34 (44.7)	34 (40.5)	0.491	0.673
ESR [mm/h]	–	–	7.5 (4.2–17.8)	8 (3.5–15.5)	20.5 (8.0–27.0)	11 (6.0–22.8)	12 (5.0–23.5)	9.5 (5.0–17.0)	**0.010**	*0.071*
CRP [mg/L]	1.4 (0.7–2.7)	1.2 (0.5–1.9)	2.8 (1.0–16.2)	1.9 (0.6–7.3)	7.6 (2.3–18.8)	6.6 (2.6–12.9)	6.1 (1.6–18.6)	4.3 (1.1–9.5)	**<0.001**	**<0.001**
ASDAS	–	–	2.2 (1.3–3.1)	1.5 (0.9–2.6)	2.4 (1.6–2.9)	2.2 (1.5–3.1)	2.3 (1.6–2.9)	1.9 (1.2–2.9)	0.866	**0.011**
Remission, n (%)	–	–	10 (26.3)	17 (40.5)	7 (18.4)	6 (13.0)	17 (22.4)	23 (26.1)	0.282	**0.034**
Low DA, n (%)	–	–	5 (13.2)	10 (23.8)	7 (18.4)	16 (34.8)	12 (15.8)	26 (29.5)		
High DA, n (%)	–	–	14 (36.8)	12 (28.6)	20 (52.6)	18 (39.1)	34 (44.7)	30 (34.1)		
Very high DA, n (%)	–	–	9 (23.7)	3 (7.1)	4 (10.5)	6 (13.0)	13 (17.1)	9 (10.2)		
BASDAI	–	–	2.9 (0.8–4.9)	2.1 (1.0–3.8)	2 (0.8–3.2)	2.1 (0.9–4.5)	2.6 (0.8–4.3)	2.1 (1.0–4.0)	0.114	0.997
Inactive or low DA, n (%)	–	–	22 (57.9)	32 (76.2)	34 (89.5)	34 (73.9)	56 (73.7)	66 (75.0)	**<0.001**	0.998
Active disease, n (%)	–	–	16 (42.1)	10 (23.8)	4 (10.5)	12 (26.1)	20 (26.3)	22 (25.0)		
BASFI	–	–	1.4 (0.3–2.6)	0.8 (0.1–3.7)	1.6 (0.6–3.2)	1.5 (0.6–3.7)	1.5 (0.5–2.9)	1.2 (0.1–3.7)	0.400	0.188
MDGAS	–	–	15 (10.0–30.0)	15 (8.8–26.2)	20 (10.0–40.0)	20 (10.0–37.8)	20 (10.0–31.2)	20 (10.0–30.0)	0.396	**0.022**
ASQoL	–	–	5 (1.0–11.8)	4 (0.0–8.0)	4.5 (2.0–9.8)	6 (2.0–11.5)	5 (1.8–10.0)	5 (1.0–10.0)	0.941	0.12
SJC	–	–	0 (0.0–0.0)	0 (0.0–0.0)	0 (0.0–0.0)	0 (0.0–0.0)	0 (0.0–0.0)	0 (0.0–0.0)	*0.092*	0.456
TJC	–	–	0 (0.0–0.0)	0 (0.0–0.0)	0 (0.0–0.0)	0 (0.0–0.0)	0 (0.0–0.0)	0 (0.0–0.0)	*0.091*	0.782

(*continued on next page*)

Table 1 (*continued*)

Characteristics	HC (n = 72)		nr-axSpA (n = 82)		r-axSpA (n = 85)		axSpA (n = 169)		p-value	
	Scr (n = 20)	Val (n = 52)	Scr (n = 38)	Val (n = 44)	Scr (n = 38)	Val (n = 47)	Scr (n = 78)	Val (n = 91)	Scr	Val
EuroQol	–	–	0.7 (0.7–0.8)	0.7 (0.7–0.8)	0.7 (0.7–0.8)	0.7 (0.6–0.8)	0.7 (0.7–0.8)	0.7 (0.6–0.8)	0.386	0.225
Enthesitis index	–	–	0 (0.0–1.0)	0 (0.0–2.0)	0 (0.0–1.0)	0 (0.0–1.0)	0 (0.0–1.0)	0 (0.0–1.0)	0.947	*0.084*
csDMARDs, n (%)	–	–	7 (18.4)	6 (13.6)	6 (15.8)	6 (13.3)	13 (17.1)	12 (13.5)	0.996	0.995
bDMARDs, n (%)	–		1 (2.6)	1 (2.4)	1 (2.6)	1 (2.2)	2 (2.6)	2 (2.2)	0.999	0.999
Glucocorticoids, n (%)	–	–	0 (0.0)	0 (0.0)	3 (7.9)	4 (8.9)	3 (3.9)	4 (4.5)	0.248	0.131
COX_2 inhibitors, n (%)	–	–	6 (15.8)	4 (9.1)	5 (13.2)	7 (15.6)	11 (14.5)	11 (12.4)	0.998	0.546
NSAIDs, n (%)	–	–	12 (31.6)	11 (25.0)	11 (28.9)	12 (26.7)	23 (30.3)	23 (25.8)	0.998	0.995
mSASSS	–	–	0 (0.0–0.0)	0 (0.0–0.0)	2 (0.0–11.6)	0 (0.0–2.5)	0 (0.0–2.0)	0 (0.0–1.75)	**<0.001**	**0.026**
ΔmSASSS	–	–	2 (1.2–2.25)	3.2 (2.4–4)	2.9 (1.3–7.5)	2 (1.75–3)	2.2 (2–3)	2 (1.2–4.4)	0.167	0.151
HLA-B27 (+), n (%)	0 (0.0)	0 (0.0)	31 (81.6)	35 (81.4)	35 (92.1)	41 (91.1)	66 (86.8)	76 (86.3)	0.319	**<0.001**

SIJ was performed for all patients diagnosed with nr-axSpA. The Spondyloarthritis Research Consortium of Canada (SPARCC) scoring system, used to evaluate BME, was applied to all available MRI examinations. The scores were assessed by an experienced rheumatologist and radiologist trained in both scoring systems, and the mean value from both assessments was used for statistical analysis [18].

2.2. Peripheral blood mononuclear cells and plasma collection

Peripheral blood samples were collected into commercially available EDTA-treated tubes, immediately centrifuged (3000×*g*/10 min), aliquoted, and stored at −80 °C until use. PBMCs were isolated from blood samples using Ficoll-Paque plus (Cytiva, Sweden, CAT: 17-1440-03), gradually centrifuged (2000×*g*/15 min/RT; then repeatedly 1000×*g*/10 min/10 °C) and stored at −80 °C until use.

2.3. Total RNA isolation

The isolation of RNA from PBMCs involved disruption of these cells using ceramic beads. Subsequently, QIAzol Lysis Reagent (Qiagen, Germany, CAT: 79306) was employed for total RNA extraction. Following the phase separation step, 100 % isopropanol was added to the collected aqueous phase and incubated for 10 min at room temperature. After centrifugation at 12,000×*g* for 10 min at 4 °C, the pellet was washed with 75 % ethanol and dissolved in RNase/DNase-free water. For the RNA quantification, we used NanoDrop 2000 (Thermo Fisher Scientific, Oregon, USA).

2.4. MPS – miRNA profiling of PBMCs

Libraries were prepared from 1 μg of total RNA using the NEXTflex Small RNA-Seq Kit v3 (Bioo Scientific, Texas, USA, CAT: NOVA-5132-06), following the manufacturer's protocol. After the amplification step, we performed a fragment analyser (Advanced Analytical) for the miRNA library (145 bp) fragment analysis and quantification. Samples were equally pooled for each particular sequencing run based on the concentration of miRNA library fragments, which were isolated using a pippin Prep instrument with 3 % agarose (Sage Science, Massachusetts, USA) before sequencing. The isolated fragments were quantified using a Qubit 2.0 fluorometer (Thermo Fisher Scientific, Oregon, USA) and subsequently used for sequencing on a NextSeq 500 (Illumina) according to the manufacturer's protocol.

2.5. Bioinformatics

Adaptor sequences were identified and removed from MPS data with the Cutadapt (v2.5) software [19]. Only high-quality reads (Phred $\geq$ ten over at least 85 % of the read length) with a length between 16 and 28 bp after adapter trimming were retained as potential miRNA reads. To assess the quality of raw and processed reads, the FastQC software was employed [20]. To prevent an increase in variance during the normalisation process, we randomly sampled 3,000,000 raw reads from each library using the seqtk toolkit before proceeding with miRNA alignment [21].

The Chimira tool [22], applied to FASTQ files, generates count-based miRNA expression data by mapping against miRBase v22 [23]. The miRNAs accounted for 1.7 million reads per sample with a balanced distribution (SD = 0.061). Only samples with a total number of aligned miRNA reads exceeding 1,000,000 were included in the evaluation of differential expression, which was performed by the DESeq method [24]. Subsequent analyses were conducted utilising R/Bioconductor packages (Supp. Table 4) [25]. Raw data and annotated sequences of the small RNA libraries have been uploaded to the GEO database.

DESeq provides an adaptive shrinkage estimator [26] for log2 fold change, which is particularly useful for miRNAs with low read count and dispersion. Additionally, the DESeq algorithm calculated the base mean, which is essentially the average of the normalised count values divided by size factors and computed across all samples. To enhance the specificity of the analysis and reduce the potential for false positives, miRNAs with a base mean > 10 were retained for further investigation. This filtering step helps exclude miRNAs that may be too low in abundance or exhibit high variability, making them difficult to distinguish from random noise. In order to identify differentially expressed miRNAs while minimising false-positives, the following criteria were applied based on the results computed by DESeq: a) an p-value <0.05; b) the base mean > 10; and c) the difference in shrunk log2 fold change (log2FC) $> |0.5|$. Alternatively, if any of the above criteria were not met for a particular miRNA, we considered its selection based on its previously established association with axSpA. Following these criteria, nine miRNAs were chosen for further validation using RT-qPCR. These miRNAs met the criteria of having a $p < 0.05$, a difference in fold change >0.5 and Ct values < 35. Importantly, each of these miRNAs was detected in at least six samples per group when comparing diagnoses. The statistical analysis for the validation data was adjusted for potential confounding variables, including sex, age, and CRP.

2.6. Quantitative real-time PCR – miRNA expression analysis

For validation of the sequencing results, the SmartChip MSND system and the SmartChip Real-Time PCR Cycler (TaKaRa, France) were utilised, ensuring high-throughput analysis, automation, and robust data reliability. Prior to the real-time PCR, samples were diluted to 1 μg of total RNA per 20-μl reaction and reversely transcribed and amplified using a TaqMan® Advanced miRNA cDNA Synthesis Kit (Thermo Fisher Scientific, Lithuania, CAT: A28007), including miR-Amp amplification. cDNA samples were stored in −20 °C. For real-time qPCR (RT-qPCR), TaqMan™ Fast Advanced Master Mix (Applied Biosystems, Lithuania, CAT: 444456), TaqMan

Advanced miRNA Assay (Applied Biosystems, Lithuania, CAT: A25576), TaqMan™ microRNA Control Assay (Applied Biosystems, Lithuania, CAT: 4427975) and SmartChip® MyDesign Kit (TaKaRa, France, CAT: 640032) were used. The protocol for SmartChip real-time PCR was pre-defined by the software. All samples and TaqMan probe combinations were analysed in tetraplicate. SmartChips represented the measurement of each sample and probe combination in tetraplicate. The Ct values were calculated using the second derivative maximum method. RNU6b was used as a reference gene. Ct values ranged from 20 to 35, and values over 35 were excluded as background noise. Relative quantification was as follows: $\Delta Ct = Ct$ (RNU-6B) – Ct (miRNA of interest). Differently expressed miRNAs were selected based on p-value <0.05 and the difference in log2FC $> |0.5|$.

2.7. Quantitative real-time PCR – cytokine expression analysis

RNAs were transcribed using High-Capacity cDNA Reverse Transcription Kit (Applied Biosystems, Lithuania, CAT: 4368814). For RT-qPCR, Quant Studio 7 (Applied, Biosystems, Lithuania), MicroAmp Fast 96-well Reaction Plates (Applied Biosystems, China, CAT: 4346907), TaqMan™ Fast Advanced Master Mix (Applied Biosystems, Lithuania, CAT: 444456) and TaqMan Gene Expression Assay (Thermo Fisher Scientific, Lithuania, CAT: 4331182) specific to the cytokines of interest, namely *IL-6, IL-17A, IL-22, IL-23A,* and *TNF*, were used. *GAPDH* was used as a reference gene. The Ct values were determined using the second derivative maximum method. Ct values ranged from 20 to 35, and values over 35 were excluded as background noise. Relative quantification was as follows: $\Delta Ct = Ct$ (GAPDH) – Ct (gene of interest).

2.8. Protein quantification

Levels of the axSpA-related cytokines (IL-6, IL-17A, IL-22, IL-23, TNF) in plasma samples were quantified using a custom multiplex immunoassay kit Bio-Plex Pro Human Th17 5-plex (Bio-Rad, California, USA, CAT: customized) according to the manufacturer's protocol. To assess the absorbance values of the cytokines, a Luminex BIO-PLEX 200 System (Bio-Rad, California, USA) was utilised. Plasma levels of TNF were measured using the Human TNF alpha ELISA Kit (RayBiotech, Georgia, USA, CAT: ELH-TNFa-1), with a sensitivity of 25 pg/mL, following the manufacturer's instructions. The quantification of IL-17 in plasma was conducted using the Human IL-17 Immunoassay Quantikine™ ELISA (R&D, Minneapolis, USA), which has a sensitivity of 15 pg/mL, in accordance with the manufacturer's protocol. Absorbance was measured at 450 nm using Spark® Multimode Microplate Reader (Tecan, Switzerland).

The study involved a total of 35 plasma samples from the screening cohort and 45 plasma samples from the validation cohort. For equal and sufficient evaluation of miRNAs expression levels across both screening and validation cohorts, a Z-score normalisation technique was applied to standardise the data. Subsequently, Kendall's tau-b correlation coefficient was calculated. The plasma levels of TNF and IL-17 were quantified in 47 nr-axSpA, 44 r-axSpA and 52 HC by ELISA.

2.9. Statistical analysis

In the miRNA screening analysis, data were processed and analysed with the RStudio software [R version 4.2.1 (2022-06-23 ucrt)] [27] and the extended R packages (Supp. Table 4) [28,29]. DESeq was employed to examine differences between two-level clinical manifestations or groups. For the ASDAS analysis, normalised read counts from DESeq were subjected to a generalized linear model with a negative binomial assumption (GLM-NB). Subsequently, pairwise follow-up comparisons were adjusted using Dunnett's test. To control for multiple testing, p-values were adjusted to Dunnett's corrections. For CRP analysis, the normalised read counts from DESeq were also analysed by GLM-NB. In both the DESeq and GLM-NB models, adjustments were made for potential confounding factors, which included sex, age, and CRP (if necessary).

In the analysis of validation data, adjustments were made for sex, age, and CRP to account for potential confounding effects. To compare differences between two-level clinical manifestations or groups, statistical tests such as unpaired *t*-test or Tukey's pairwise comparisons were used.

In screening and validation cohorts, we applied linear modelling to find the associations between cytokines gene expressions and miRNA expressions.

2.10. miRNA-target and pathway enrichment analyses

MIENTURNET tools were applied to investigate putative miRNA-mRNA targets and pathways affected by miRNAs with altered regulation [30].

3. Results

3.1. Clinical characteristic

Clinical and demographic characteristics are shown in Table 1, describing the cohort of axSpA patients, which was further classified into nr-axSpA and r-axSpA. In the r-axSpA subgroup, there was a notable increase in disease activity, which was demonstrated by a range of clinical and laboratory indicators, such as ESR, CRP, ASDAS, and MDGAS. Patients in the r-axSpA subgroup were more frequently HLA-B27 positive compared to the nr-axSpA subgroup. As expected, the mSASSS was higher in the r-axSpA subgroup, which is in line with previous findings [31]. Over two years, 15.4 % of patients demonstrated progression of spinal involvement as assessed by

changes in mSASSS. The majority of patients were in the early stages of their disease and predominantly naïve to bDMARDs therapy, with 12.6 % initiating bDMARDs treatment over the course of two years. The correlation matrix illustrating the relationship between various laboratory and clinical parameters is shown in Supplementary Fig. 1.

3.2. Whole miRNome sequencing of PBMCs

In our study, we focused on the PBMCs miRNA profiles of patients with nr-axSpA, r-axSpA, and HC aiming to identify miRNAs that are expressed differently across these groups. MiRNA sequencing data was aligned to the miRBase database, resulting in the identification of a total of 1900 miRNAs in all samples. For subsequent analysis, only 432 miRNAs with adequate read counts (at least 10 raw reads in 1/3 of all samples) were included. As a result, we found 48 miRNAs with an altered expression when comparing axSpA patients ($n = 76$) with HC ($n = 20$) (Fig. 1). Additionally, 42 miRNAs exhibited altered expression when comparing patients with different disease activity levels based on ASDAS (Supp. Tables 3 and 4). Notably, 10 (miR-96-5p, miR-144-3p, miR-145-3p, miR-154-3p, miR-182-5p, miR-183-5p, miR-199b-5p, miR-451a, miR-486-5p, miR-582-5p). miRNAs were dysregulated simultaneously when comparing axSpA patients with HC and were also associated with the ASDAS score (Fig. 2C; Supp. Table 3). The difference in log2FC and direction and p-value are depicted in volcano plots (Fig. 2B).

Principal Component Analysis (PCA) was utilised to visualise the expression pattern of individual samples. The plot in Fig. 2B suggests that there are similar expression patterns among the different subgroups, indicating a resemblance in miRNA expressions in PBMCs across the cohorts. Despite the overall similarity in miRNA expression pattern, the analysis identified 25 miRNAs that were suitable for distinguishing between patients with nr-axSpA and r-axSpA (Supp. Table 1.). Of these, 12 miRNAs were validated. The remaining 13 miRNAs showed no differential expression when compared to HC, nor did they indicate any association with ASDAS.

3.3. miRNA expression validation

For the validation analysis, we selected 45 miRNAs through a screening process. Initially, 432 miRNAs were detected and reduced to 90 miRNAs based on the following criteria: a) $p < 0.05$ and b) BaseMean >10. Subsequently, we applied additional criteria to these 90 miRNAs, selecting those with c) a log2 fold change (log2FC) $> |0.5|$, d) no outliers, and e) low variance and support in the literature. This rigorous process resulted in the selection of 45 miRNAs for further analysis (Fig. 1).

In our validation analysis (Fig. 3, Supp. Fig. 2), three miRNAs had altered expression profiles. First, miR-1248 exhibited decreased expression ($p = 0.003$, $\Delta Ct = -1.125$) in axSpA patients compared to HC (Fig. 2D). Second, miR-1246 was also downregulated in axSpA patients during validation ($p = 0.047$, $\Delta Ct = -0.645$). Finally, miR-1-3p was found to be upregulated in axSpA patients compared to HC during validation ($p = 0.006$, $\Delta Ct = 1.757$).

However, several miRNAs were excluded from further analysis for various reasons. MiR-619-5p and miR-1299 were eliminated due to the presence of many outliers, which could affect the reliability of the results. Although miR-182-5p and miR-223-3p were significantly different between axSpA and HC, they were omitted from the analysis because they showed opposite directions of regulation in the screening and validation experiments.

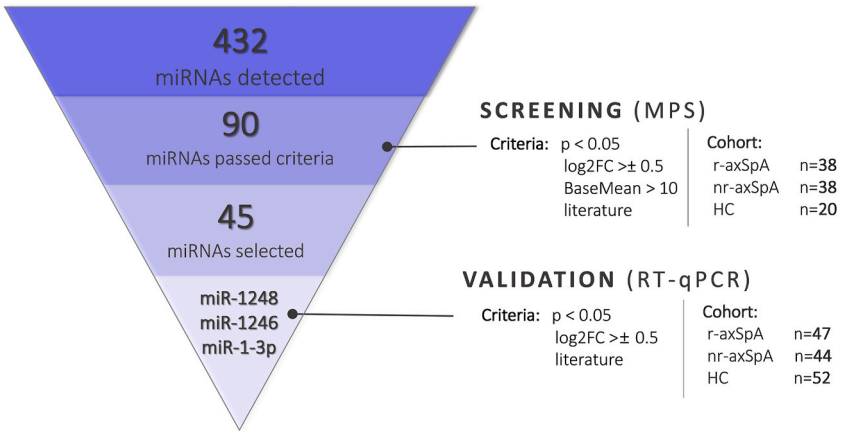

Fig. 1. Workflow and criteria for miRNA selection. Abbreviations: ASDAS, Ankylosing Spondylitis Disease Activity Score; ASQoL, Ankylosing Spondylitis Quality of Life; BASDAI, Bath Ankylosing Spondylitis Disease Activity Index; BASFI, Bath Ankylosing Spondylitis Functional Index; Chin-to-chest, Measurement for spinal mobility; CRP, C-reactive protein; Enthesitis index, Index measuring enthesitis; ESR, Erythrocyte sedimentation rate; EuroQoL, European Quality of Life; HAQ, Health Assessment Questionnaire; HLA-B27, Human leukocyte antigen B27; IL-6, Interleukin 6; IL-17, Interleukin 17; IL-22, Interleukin 22; IL-23, Interleukin 23; MDGAS, Modified Disease Global Assessment Scale; mSASSS, Modified Stoke Ankylosing Spondylitis Spine Score; nr-axSpA, Non-radiographic axial spondyloarthritis; Occiput-to-wall, Measurement for spinal mobility; PBMC, Peripheral blood mononuclear cells; qPCR, Quantitative Polymerase Chain Reaction; r-axSpA, Radiographic axial spondyloarthritis; Schober test, Test for spinal mobility; SPARCC, Spondyloarthritis Research Consortium of Canada; TNF, Tumor necrosis factor; VAS, Visual Analogue Scale.

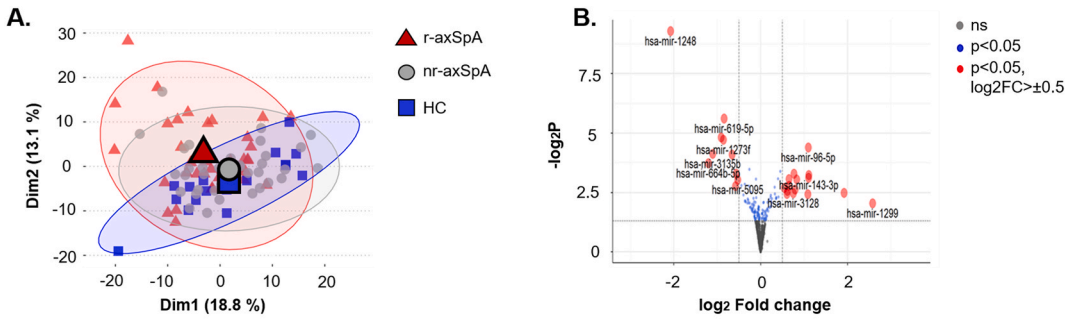

C.

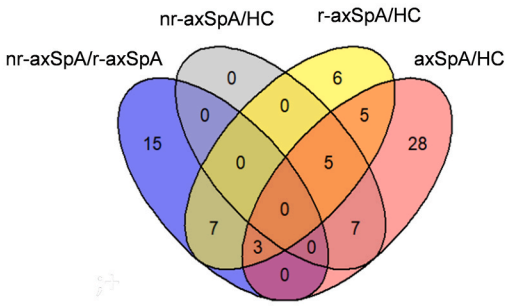

D.

miRNA	Screening		Validation	
	log2FC	p-value	ΔCt	p-value
axSpA vs. HC				
miR-1-3p	**0.5**	**0.082**	**1.757**	**0.006**
miR-1246	**-1.304**	**0.046**	**-0.645**	**0.047**
miR-1248	**-1.813**	**<0.001**	**-1.125**	**0.003**
miR-1299	3.241	<0.001	1.025	0.051
miR-619-5p	-0.802	<0.001	-1.677	0.002
miR-223-3p	0.251	0.057	-0.655	0.048
miR-182-5p	0.339	0.135	-1.337	0.051
miR-191-5p	-0.031	0.766	2.601	0.011
miR-25-3p	0.053	0.544	1.068	0.011
let-7b-5p	0.109	0.311	-0.769	0.027
miR-16-2-3p	0.005	0.952	-0.851	0.035
nr-axSpA vs. r-axSpA				
miR-1246	-1.732	<0.001	0.792	0.146
miR-199b-5p	-0.457	0.002	1.202	0.078
miR-582-5p	-0.472	0.026	0.847	0.033

Fig. 2. The characteristics of the miRNome screening data are depicted as follows: (A) Principal component analysis (PCA) shows the data distribution in the screening cohort indicating the minor differences between subgroups. Data for r-axSpA, nr-axSpA, and HC are represented with triangles, circles, and squares, respectively; The subgroups are colour-coded, with r-axSpA in red, nr-axSpA in grey, and HC in blue. (B) miRNAs distribution in the screening cohort. Red points indicate miRNAs that are either downregulated or upregulated ($p < 0.05$, differences in log2FC> ±0.5). Blue points represent miRNAs that did not meet the log2FC criterion, while grey points represent statistically nonsignificant data. (C) Venn's diagram illustrates the differently expressed miRNAs in the screening cohort. Comparisons between groups are as follows: nr-axSpA versus r-axSpA, nr-axSpA versus HC, r-axSpA versus HC, axSpA versus HC, and ASDAS. (D) List of dysregulated miRNAs in the screening and validation cohorts, along with their log2 fold-change (log2FC) and p-values. The estimated means were adjusted for age, sex, and CRP in both the screening and validation cohorts. The p-values indicate statistical significance between axSpA patients and HC, unless otherwise specified. P-values were computed using GLM-NB with Dunnett's correction in the screening analysis and ANOVA with Tukey's test in the validation analysis. Statistically significant differences ($p < 0.05$) are highlighted in bold. Abbreviations: ANOVA, Analysis of Variance; AxSpA, Axial Spondyloarthritis; HC, Healthy Controls; nr-axSpA, Non-Radiographic axSpA; r-axSpA, Radiographic axSpA.

3.4. miRNA expression and disease activity, structural damage and subtypes

We conducted Tukey's pairwise comparison, which revealed that none of the miRNAs selected for validation could distinguish between the radiographic and non-radiographic subtypes of axSpA.

We also examined the relationship of validated miRNAs with other clinically relevant parameters including systemic inflammation (ESR, CRP) and local inflammation (SPARCC), disease activity (ASDAS, BASDAI), function and other patient reported outcomes (BASFI, ASQoL, EuroQol, HAQ), structural damage, including radiographic progression (mSASSS, ΔmSASSS). However, none of these miRNAs demonstrated significant associations in axSpA patients with these clinically relevant parameters in both the screening and validation phases (Fig. 4). Furthermore, patients undergoing treatment with NSAIDs exhibited reduced levels of miR-1-3p, while those receiving csDMARDs therapy demonstrated decreased levels of miR-1248. We observed differences in miR-1248 expression between HC and patients in remission, as well as between HC and patients with high disease activity. However, since the miR-1248 expression levels in patients with low disease activity and those with very high disease activity were comparable to those in HC, we were unable to establish a definitive association between miR-1248 expression and disease severity.

3.5. miR-1-3p and miR-1248 are associated to IL-6 gene expression

Initially, we investigated the gene expression of *IL-6, IL-17, IL-22, IL-23*, and *TNF*. While these cytokines are known to play significant roles in inflammatory processes, we found that the gene expression was not significantly different between axSpA patients and HC. However, it is worth noting that IL-23 was downregulated in axSpA patients compared to HC ($p = 0.009$, log2FC = 0.607) in the

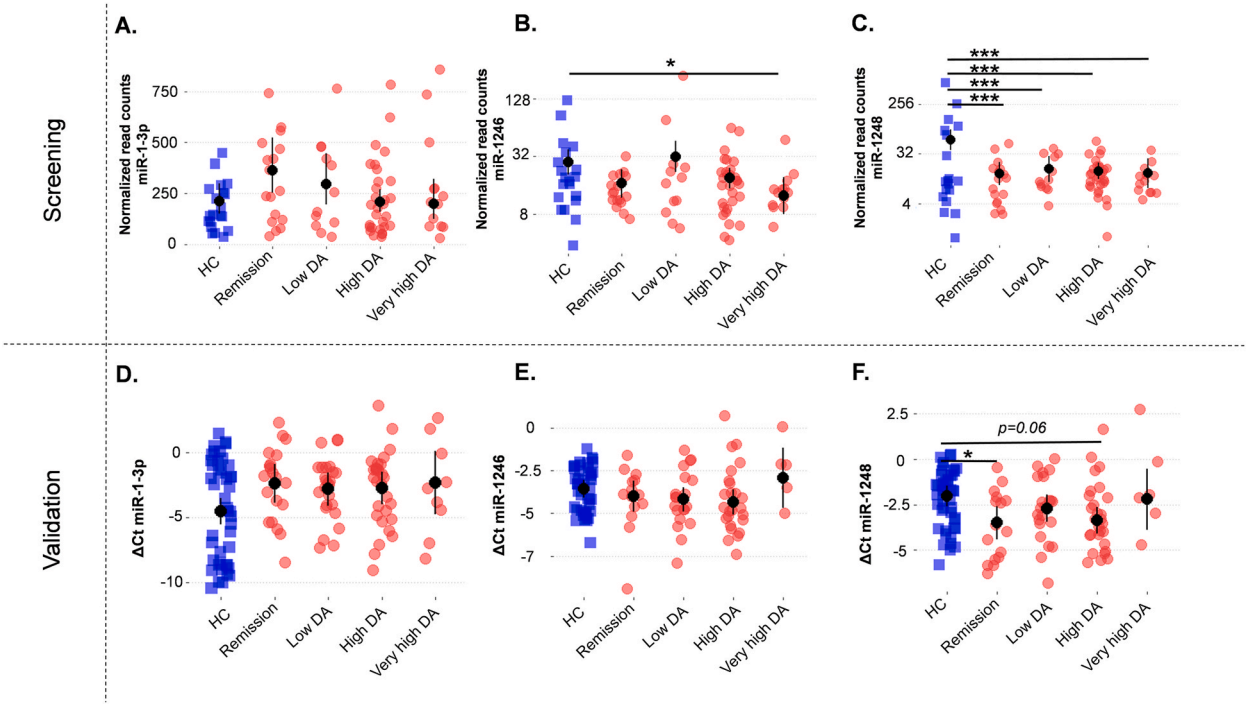

Fig. 3. Gene expression of candidate miRNAs in patients with different disease activity grades, as determined by the ASDAS score. The error bars represent 95 % confidence intervals with the estimated mean. The estimated means and error bars were adjusted for age, sex, and CRP in both screening and validation. The p-values show statistical significance between healthy controls (HC) and grades of axSpA (remission, low disease activity (DA), high DA, very high DA) and were computed using ANOVA Significant differences are marked by asterisks. *$p < 0.05$; ***$p < 0.001$.

validation cohort, although this difference was not observed in the screening phase (Supp. Fig. 3). Interestingly, gene expression of *IL-17* and *IL-22* was undetectable in PBMCs using RT-qPCR.

In the validation cohort, we identified an association between miR-1-3p and miR-1248 and the gene expression of *IL-6* (Fig. 5). Specifically, miRNA-1-3p was positively associated with *IL-6* gene expression ($p = 0.039$, $\beta = 0.665$), while miR-1248 was negatively associated with *IL-6* gene expression ($p < 0.001$, $\beta = 0.207$). We did not identify any association of validated miRNAs with *IL-17, IL-22, IL-23* or *TNF* gene expression.

3.6. *miR-1-3p is positively associated with plasma levels of IL-17 and TNF*

We observed increased plasma levels of IL-6 in patients with axSpA (r-axSpA, n = 27; nr-axSpA, n = 27) compared to HC (n = 26) [median (IQR): 3.3 (2.0–7.2) vs 1.8 (1.2 3.1) ng/mL, p = 0.0015]. There was a trend towards an increase in IL-23 levels [329 (279–376) vs 234 (187–413) ng/mL, p = 0.07) and a decrease in IL-22 levels [10.7 (7.3–18.0) vs 14.3 (4.1–18.0) ng/mL, p = 0.092] in patients with axSpA compared to HC. There were no significant differences in plasma levels of IL-17 or TNF levels between axSpA patients and HC (Supp. Fig. 4). See the correlation matrix (Supp. Fig. 1).

Additionally, miR-1-3p positively associated with plasma levels of IL-17 ($p = 0.016$, $\tau = 0.244$) and TNF ($p = 0.028$, $\tau = 0.216$) (Fig. 6). There were no other significant associations observed between validated miRNAs and the selected cytokines in plasma.

Plasma levels of TNF and IL-17 were validated by ELISA across the cohort, [r-axSpA (n = 44), nr-axSpA (n = 44), and HC (n = 52)] and a significant difference was observed in TNF levels between the r-axSpA and HC groups [54.892 (41.7–71.5) vs. 43.374 (20.8–56.8) pg/mL, p = 0.011], after adjusting for sex and age. No significant difference in TNF concentration was found between the nr-axSpA group [42.281 (30.9–63.3) pg/mL] and HC. IL-17 levels were similar between the groups [r-axSpA: 49.827 (30.6–76.1) pg/mL; nr-axSpA: 38.057 (22.9–67.1) pg/mL; HC: 18.781 (14.7–22.6) pg/mL]. However, samples under the lower detection limit were excluded from the analysis, reducing the sample sizes to HC (n = 4), r-axSpA (n = 31), and nr-axSpA (n = 26). Additionally, a positive association between miR-1-3p and TNF was identified ($p = 0.031$, $\beta = 2.193$), with a positive trend observed for IL-17 ($p = 0.059$, $\beta = 1.932$) (Fig. 6).

3.7. *Functional enrichment analysis*

To identify miRNA-target interactions and the pathways affected by the validated miRNAs, we employed the MIENTURNET tool [30]. MiR-1-3p targets *IL-6* and, through its regulation, is also implicated in the *IL-17* and *TNF* signalling pathways. The enrichment analysis (Supp. Fig. 5) revealed a significant link between miR-1-3p processes related to bone remodelling and extracellular matrix

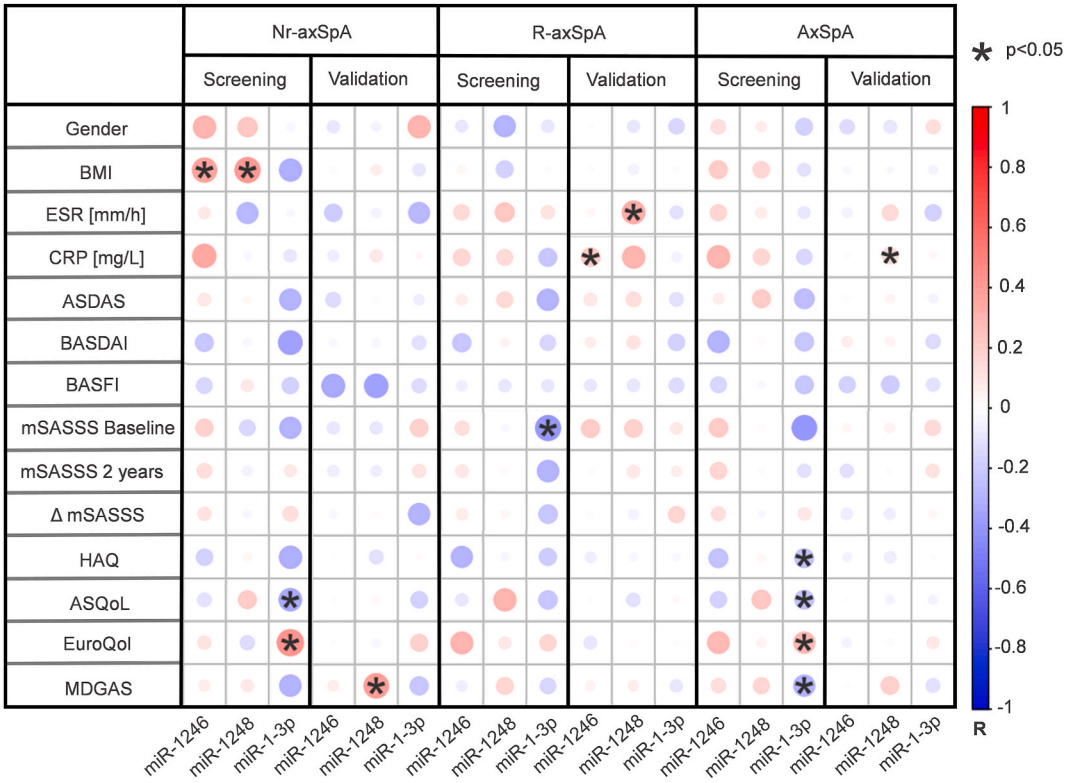

Fig. 4. Correlation matrix of validated miRNAs miR-1246, miR-1248, and miR-1-3p with clinically relevant parameters in axSpA patients in screening and validation phase. Bivariate analysis was computed using the Spearman test. R-value is depicted as a circle shaped and coloured according to the scale, p-value <0.05 is depicted as an asterisk. Abbreviations: ASDAS, The Ankylosing Spondylitis Disease Activity Score; Asqol, Ankylosing Spondylitis Quality Of Life; Axspa, Axial Spondyloarthritis; BASDAI, The Bath Ankylosing Spondylitis Disease Activity Index; BASFI, Bath Ankylosing Functional Index; BMI, Body Mass Index; CRP, C-Reactive Protein; ESR, Erythrocyte Sedimentation Rate; EuroQol, European Quality of Life; HAQ, Health Assessment Questionnaire; MDGAS, medical doctor global assessment of disease activity; mSASSS, Modified Stoke Ankylosing Spondylitis Spinal Score; Nr-Axspa, Non-Radiographic AxSpA; R-Axspa, Radiographic AxSpA.

interactions. Furthermore, the analysis indicated a significant association between miR-1246 and calcium-dependent events. Although miR-1248 does not target *IL-6*, database analysis identified a significant connection between miR-1248 and the *JAK/STAT* signalling pathways.

4. Discussion

In this comprehensive study, we conducted an in-depth analysis of the miRNome in PBMCs derived from axSpA patients and HC to reveal specific miRNAs and elucidate their association with pro-inflammatory cytokines, axSpA disease activity and spinal involvement. We identified and validated the altered expression of specific miRNAs, namely miR-1-3p, miR-1248, and miR-1246, in axSpA patients compared to HC. Nonetheless, our investigation did not reveal miRNAs capable of differentiating between non-radiographic and radiographic disease subtypes of axSpA.

Additionally, we did not observe a significant relationship between cellular miRNAs and clinical parameters such as disease activity and spinal involvement. However, we identified an association between miR-1-3p and pro-inflammatory cytokines, specifically IL-17 and TNF. Correspondingly, patients undergoing NSAIDs therapy exhibited decreased levels of miR-1-3p. This finding suggests a potential role of miRNAs in modulating the pro-inflammatory pathways implicated in axSpA.

Numerous studies have focused on the differences between r-axSpA and nr-axSpA; however, none have delineated a clear clinical picture in both axSpA subsets [3,4]. In our study, we conducted a comprehensive profiling of the miRNome within PBMCs with the aim of identifying miRNAs that are specific to patients with r-axSpA or nr-axSpA. PCA of the miRNome suggests a resemblance between both axSpA subtypes. Consequently, our analysis revealed 25 miRNAs that could distinguish patients with r-axSpA from healthy controls. However, we did not identify any miRNA that could be specifically attributed to nr-axSpA. The validation analysis corroborated the differential expression of three miRNAs in patients with axSpA in comparison to healthy individuals. Nevertheless, none of these miRNAs exhibited the capacity to differentiate between the radiographic and non-radiographic subtypes. Remarkably, our findings align with those of Li et al., who reported similar miRNA expression profiles in PBMCs from patients with nr- and r-axSpA and HC using miRNA microarray and RT-qPCR [32]. This study used MPS, which can provide superior sensitivity and specificity,

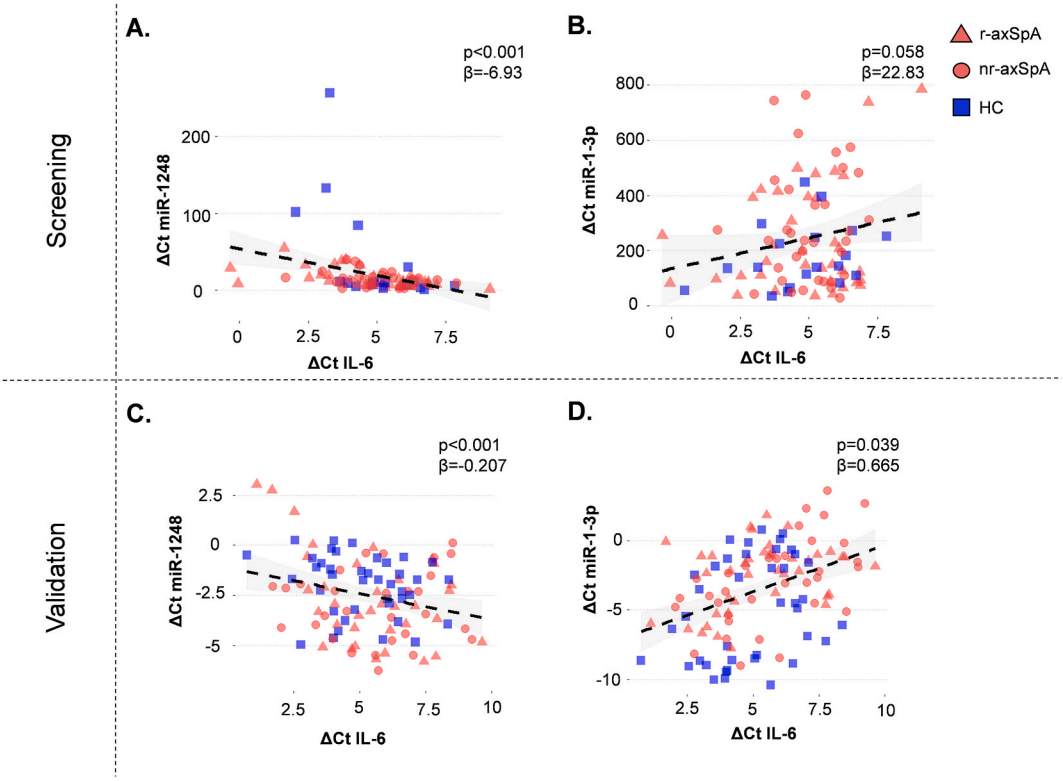

Fig. 5. Associations of candidate miRNAs with gene expressions of IL-6 in PBMCs in axSpA patients and HC. (A) miR-1248 is negatively associated with IL-6 expression in the screening cohort ($p < 0.001$, $\beta = -6.93$). (B) miR-1-3p is positively associated with IL-6 expression in the screening cohort ($p = 0.058$, $\beta = -22.83$). (C) miR-1248 is negatively associated with IL-6 expression in the validation cohort ($p < 0.001$, $\beta = -0.207$). (D) miR-1-3p is positively associated with IL-6 expression in the validation cohort ($p = 0.039$, $\beta = 0.665$). The regression lines were computed using GLM-NB and regression models in screening and validation, respectively; adjusted for age, sex, and CRP, presented with 95 % confidence intervals. Data for r-axSpA and nr-axSpA are represented with triangles and circles, respectively; axSpA and healthy controls are colour-coded in red and blue, respectively. Abbreviations: GLM-NB, Negative Binomial Generalized Linear Model; HC, Healthy Controls; IL, Interleukin; nr-axSpA, Non-Radiographic Axial Spondyloarthritis; PBMCs, Peripheral Blood Mononuclear Cells; r-axSpA, Radiographic Axial Spondyloarthritis.

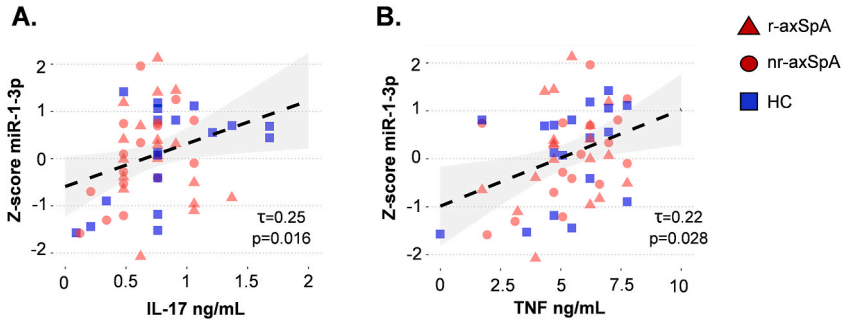

Fig. 6. The association of miR-1-3p with the plasma levels of IL-17 and TNF. (A) miR-1-3p is positively associated with IL-17 ($p = 0.016$, $\tau = 0.25$). (B) miR-1-3p is positively associated with TNF ($p = 0.028$, $\tau = 0.22$). The Y-axis represents the Z-score of miR-1-3p for equal and sufficient evaluation of miRNAs expression levels from both screening and validation cohorts. (C) miR-1-3p is positively associated with IL-17 ($p = 0.059$, $\beta = 1.932$). (D) miR-1-3p is positively associated with TNF ($p = 0.031$, $\beta = 2.193$). The regression lines were computed using regression models adjusted for age, sex, and CRP, presented with 95 % confidence intervals. Data for r-axSpA and nr-axSpA are represented with triangles and circles, respectively; axSpA and healthy controls are colour-coded in red and blue, respectively. Abbreviations: CRP, C-Reactive Protein; HC, Healthy Controls; IL, Interleukin; nr-axSpA, Non-Radiographic Axial Spondyloarthritis; r-axSpA, Radiographic Axial Spondyloarthritis; TNF, tumour necrosis factor.

allowing for the detection of low-abundance transcripts and the discovery of novel miRNAs that microarray RNA cannot identify. Moreover, miRNA microarrays rely on predesigned probes, which may not accurately reflect the complete miRNA profile in the sample. On the other hand, our previous work highlighted miR-625-3p as a potential biomarker, given its elevated expression in nr-axSpA compared to HC. However, it is important to note that our previous study focused on circulating miRNAs and profiled plasma samples [12]. In contrast to these earlier endeavours, the results of our current study offer heightened precision, as miRNAs dysregulation has been verified through two distinct methods within a larger cohort. Screening of PBMCs is advantageous for miRNA expression analysis due to their stability, specificity, and ability to reduce variability and confounding effects compared to plasma samples [33,34]. In our study, we observed upregulated miR-1-3p expression in patients with axSpA. We hypothesise that this upregulation may be linked to processes related to bone remodelling and interactions within the extracellular matrix. Notably, miR-1-3p has putative targets, including Secreted Frizzled-Related Protein (*SFRP1*), and reduced miR-1-3p expression has been associated with suppression of bone formation and osteoblasts maturation [35]. Furthermore, the silencing of miR-1-3p in cartilage has been shown to lead to the downregulation of key factors such as *RUNX2* and *type X collagen*, along with the upregulation of *SOX9*. These changes can result in developmental dysplasia of the hip [36,37]. In contrast, the introduction of miR-1 3p mimics has been found to promote the expression of factors like alkaline phosphatase (*ALP*), calcifications and osteogenic markers (*RUNX2, OPN, OCN, OSX*), facilitating osteoblast differentiation and maturation [38]. Overall, these results suggest a protective role of miR-1-3p against destructive bone damage and indicate its potential involvement in the pathogenesis of axSpA. Importantly, our data revealed a positive association between miR-1-3p and plasma levels of IL-17 and TNF. These cytokines are known mediators of bone destruction, suggesting the activation of defense mechanisms in axSpA patients [39]. The positive association between miR-1-3p and cellular *IL-6* gene expression corresponds with the reduction of miR-1-3p levels in patients undergoing NSAIDs therapy, suggesting a link between miR-1-3p and inflammatory processes.

We found a downregulation of miR-1248 in axSpA patients that was negatively associated with the gene expression of *IL-6* in axSpA patients and HCs. However, alleviation in miR-1248 levels was also observed in patients undergoing csDMARDs therapy suggesting a potential impact on *IL-6* gene expression. Notably, a recent study found an association between miR-1248 and the *JAK/STAT* signalling pathway, which plays a pivotal role in immune-mediated inflammatory diseases, including axSpA. This study revealed a suppressive effect of miRNA-1248 on the production of interferon (IFN)-β, a ligand involved in the *JAK/STAT* signalling [40]. However, this inhibitory function of miR-1248 can be counteracted by hsa_circRNA_008961, a circular RNA that was found to be highly upregulated in PBMCs and associated with inflammation in active r-axSpA [41]. Our pathway prediction analysis further supports these findings by suggesting that miR-1248 may target *IL-5*, a cytokine that is upregulated in r-axSpA [42], as well as *IL-2Rα* (IL-2 receptor alpha chain, *CD25*), which is expressed on the cell surface of IL-17–producing γδ T cells [43]. These results, in conjunction with our data, are consistent with the literature and indicate a disruption of the functional role of miR-1248 in r-axSpA.

The expression of miR-1246 exhibited a significant distinction between radiographic and non-radiographic subtypes in the screening cohort; however, this differentiation could not be confirmed in the subsequent validation cohort. In the latter, miR-1246 was only able to differentiate between axSpA patients and HC. This discrepancy in findings may be attributed, in addition to several acknowledged biases, to the low sensitivity of RT-qPCR compared to MPS, which was used in the screening cohort [44]. Nonetheless, miR-1246 emerges as a potentially significant player in the pathogenesis of axSpA, as it has been shown to target components of inflammatory pathways and osteoblast differentiation (e.g. calmodulin, p53, SP7) [45]. Calmodulin 2, in particular, is known to stimulate the synthesis of pro-inflammatory cytokines (IL-6, IL-1, and TNF) through the activation of calcium/calmodulin-dependent kinases and NF-κB [46]. Furthermore, the positive association between miR-1246 and SP7 (Sp Transcription Factor) suggests their potential involvement in bone remodelling activities [45]. Notably, significant dysregulation of miR-1246 expression has also been observed in other musculoskeletal conditions such as osteoarthritis [47], rheumatoid arthritis [48], and systemic lupus erythematosus [49]. These findings underscore the potential relevance of miR-1246 in the context of various rheumatic diseases and its intricate role in modulating inflammatory and bone-related pathways.

Inflammation plays a pivotal role in the pathogenesis of axSpA, prompting numerous studies to investigate changes in cytokines, including IL-17, IL-23 and TNF, in various biological materials [50]. These cytokines have become targets for therapeutic interventions in the treatment of axSpA. Among the pro-inflammatory cytokines studied, therapies focused on blocking IL-6 or IL-23 have shown limited efficacy [51], while inhibitors targeting TNF and IL-17 have proven to be effective in axSpA patients [52]. Therefore, we investigated the gene expression of selected pro-inflammatory cytokines in PBMCs and measured their concentrations in the bloodstream. At the cellular level, expressions of *IL-6, -17, -22, -23*, and *TNF* were found to be indistinguishable in axSpA patients. This lack of distinction may be attributed to the heterogeneity within the cell population, with varying expression profiles in different cell types such as lymphocytes or monocytes [42]. Additionally, it is worth noting that differences in disease duration among patients may also contribute to the observed variability in cytokine expressions. In contrast, we observed elevated plasma IL-6 concentrations. However, it is important to recognise that plasma circulates throughout the body, and its content may not necessarily provide a reliable basis for comparing tissue-specific disease characteristics [53]. These findings highlight the complexity of cytokine regulation and distribution in axSpA and emphasise the importance of considering both tissue-specific and systemic factors in the evaluation of inflammatory responses.

This study has several advantages. We enrolled 167 axSpA patients (further classified as non-radiographic or radiographic axSpA), each with well-defined disease activity based on CRP, ASDAS, and radiographs over two years. In addition, our comprehensive clinical assessments included an extended subset of parameters enabling a detailed examination of disease activity. The use of the SmartChip method in our study eliminated technical biases in the results, a challenge that can occur when multiple samples or assays are being processed. However, it is important to acknowledge that while we carefully selected specific miRNAs for validation, there remains the possibility that some significant miRNAs may have escaped our attention. Furthermore, it should be noted that RT-qPCR has

limitations, particularly in its ability to identify miRNAs with low expression levels (Ct > 35). We observed notable variability in miRNA profiles when employing the two-method miRNA profiling approach. This variability may be attributed to the inherent heterogeneity of the cell population within PBMCs and the complex regulatory dynamics of miRNAs, or/and different sensitivity of used methods. Also, the inclusion of two patient cohorts introduces another variable that could account for the observed differences. To account for potential confounding factors, our results were rigorously adjusted for CRP, sex, and age, as these variables can influence miRNA expression. While no association was observed between validated miRNAs and patient therapy, it is important to note that we cannot definitively exclude the possibility of therapy's effect on gene expression. During the two-year follow-up of our study, a total of 21 patients commenced treatment with bDMARDs, potentially influencing the mSASSS score. However, the exclusion of these patients from our analysis did not significantly alter the outcomes of the study. The identified associations of differentially expressed miRNAs with clinically relevant parameters do not establish causality, confirmation through functional experiments is essential to elucidate any causal relationships. Finally, while our study has provided valuable insights, it is essential to acknowledge that further validation in an extended cohort is warranted to strengthen the robustness and generalizability of our findings.

5. Conclusions

This study underscores the dysregulation of miR-1-3p, miR-1246, and miR-1248 in axSpA, a notion reinforced by recent research findings. While our study did not identify specific miRNAs unique to axSpA subtypes and did not establish correlations between cellular miRNAs, disease activity, or spinal involvement, including radiographic progression, the association between miR-1-3p, IL-17, and TNF suggests a potential role for miR-1-3p in the pathogenesis of axSpA. In conclusion, this study adds another piece to the complex puzzle of miRNA involvement in axSpA and sheds light on the dysregulation of these specific miRNAs and their potential importance in the disease process.

Funding

This study was supported by Research project No. 023728 of the Ministry of Health of the Czech Republic, BBMRI-CZ LM2018125, and Charles University project SVV 260 638.

Ethics statement

The studies involving human participants were reviewed and approved by the Institutional Ethics Committee of the Institute of Rheumatology, Prague, Czech Republic (ID: 7117/2018). Informed consent was obtained from all subjects involved in the study.

Data availability statement

Raw data and annotated sequences of the small RNA libraries have been uploaded to the GEO database (Accession ID: GSE252708).

CRediT authorship contribution statement

Aneta Prokopcova: Writing – original draft, Visualization, Validation, Software, Methodology, Investigation, Formal analysis, Data curation. **Jiri Baloun:** Writing – review & editing, Validation, Supervision, Software, Methodology, Formal analysis, Data curation, Conceptualization. **Kristyna Bubova:** Writing – review & editing, Resources, Methodology. **Monika Gregova:** Resources. **Sarka Forejtova:** Resources. **Jana Horinkova:** Resources. **Marketa Husakova:** Resources. **Katerina Mintalova:** Resources. **Vladimir Cervenak:** Methodology. **Michal Tomcik:** Resources. **Jiri Vencovsky:** Resources. **Karel Pavelka:** Resources. **Ladislav Senolt:** Writing – review & editing, Validation, Supervision, Resources, Project administration, Funding acquisition, Conceptualization.

Declaration of competing interest

The authors declare that the research was conducted in the absence of any commercial or financial relationships that could be construed as a potential conflict of interest.

Acknowledgments

We would like to thank Xiao Svec for the language editing of our manuscript.

List of abbreviations

ALP	Alkaline Phosphatase
AS	Ankylosing Spondylitis
ASDAS	Ankylosing Spondylitis Disease Activity Score
ASAS	Assessment of Spondyloarthritis International Society
ASQoL	Ankylosing Spondylitis Quality of Life

axSpA Axial Spondyloarthritis
BASDAI Bath Ankylosing Spondylitis Disease Activity Index
BASFI Bath Ankylosing Spondylitis Functional Index
bDMARDs Biological Disease-Modifying Anti-Rheumatic Drugs
BMI Body Mass Index
BME Bone Marrow Edema
CRP C-Reactive Protein
csDMARDs Conventional Synthetic Disease-Modifying Anti-Rheumatic Drugs
Ct Cycle Threshold
DA Disease Activity
ΔCt Delta Cycle Threshold
ESR Erythrocyte Sedimentation Rate
EDTA Ethylenediaminetetraacetic Acid
EuroQoL European Quality of Life
GAPDH Glyceraldehyde 3-Phosphate Dehydrogenase
GLM-NB Generalized Linear Model with Negative Binomial Assumption
HC Healthy Controls
IFN Interferon
IL Interleukin
IQR Interquartile Range
JAK/STAT Janus Kinase/Signal Transducer and Activator of Transcription
log2FC log 2 Fold Change
MDGAS Medical Doctor Global Assessment
MIENTURNET miRNA Enrichment Turn Network Tool
MRI Magnetic Resonance Imaging
miRNAs MicroRNAs
MPS miRNA Profiling of PBMCs
mSASSS Modified Stoke Ankylosing Spondylitis Spinal Score
nr-axSpA Non-Radiographic Axial Spondyloarthritis
NSAIDs Non-Steroidal Anti-Inflammatory Drugs
OCN Osteocalcin
OPN Osteopontin
OSX Osterix
PBMCs Peripheral Blood Mononuclear Cells
r-axSpA Radiographic Axial Spondyloarthritis
RNA Ribonucleic Acid
RT Room Temperature
RT-qPCR Real-Time Quantitative Polymerase Chain Reaction
RUNX2 Runt-Related Transcription Factor 2
SFRP1 Secreted Frizzled-Related Protein 1
Scr Screening
SIJ Sacroiliac Joints
SJC Swollen Joint Count
SOX9 SRY-Box Transcription Factor 9
SP7 Sp7 Transcription Factor
SPARCC Spondyloarthritis Research Consortium of Canada
TJC Tender Joint Count
TNF Tumor Necrosis Factor
Val Validation

Appendix A. Supplementary data

Supplementary data to this article can be found online at https://doi.org/10.1016/j.heliyon.2024.e38250.

References

[1] M. Rudwaleit, et al., The development of Assessment of SpondyloArthritis international Society classification criteria for axial spondyloarthritis (part II): validation and final selection, Ann. Rheum. Dis. 68 (6) (2009) 777–783, https://doi.org/10.1136/ard.2009.108233.

[2] M. Rudwaleit, et al., The early disease stage in axial spondylarthritis: results from the German spondyloarthritis inception cohort, Arthritis Rheum. 60 (3) (2009) 717–727, https://doi.org/10.1002/art.24483.
[3] C. López-Medina, A. Molto, P. Claudepierre, M. Dougados, Clinical manifestations, disease activity and disease burden of radiographic versus non-radiographic axial spondyloarthritis over 5 years of follow-up in the DESIR cohort, Ann. Rheum. Dis. (2019) 209–216, https://doi.org/10.1136/annrheumdis-2019-216218.
[4] K. Bubová, et al., Cross-sectional study of patients with axial spondyloarthritis fulfilling imaging arm of ASAS classification criteria: baseline clinical characteristics and subset differences in a singlecentre cohort, BMJ Open 9 (4) (2019) 1–6, https://doi.org/10.1136/bmjopen-2018-024713.
[5] F. Costantino, N. Zeboulon, R. Said-Nahal, M. Breban, Radiographic sacroiliitis develops predictably over time in a cohort of familial spondyloarthritis followed longitudinally, Rheumatology 56 (5) (2017) 811–817, https://doi.org/10.1093/rheumatology/kew496.
[6] D. Poddubnyy, et al., Rates and predictors of radiographic sacroiliitis progression over 2 years in patients with axial spondyloarthritis, Ann. Rheum. Dis. 70 (8) (2011) 1369–1374, https://doi.org/10.1136/ard.2010.145995.
[7] E.M. Gravallese, G. Schett, Effects of the IL-23–IL-17 pathway on bone in spondyloarthritis, Nat. Rev. Rheumatol. 14 (11) (2018) 631–640, https://doi.org/10.1038/s41584-018-0091-8.
[8] A. Pekáčová, J. Baloun, X. Švec, L. Šenolt, Non-coding RNAs in Diseases with a Focus on Osteoarthritis, Wiley Interdiscip. Rev. RNA, July, 2022, https://doi.org/10.1002/wrna.1756.
[9] K. Prajzlerová, L. Šenolt, M. Filková, Is there a potential of circulating miRNAs as biomarkers in rheumatic diseases? Genes Dis 10 (4) (2023) 1263–1278, https://doi.org/10.1016/j.gendis.2022.08.011.
[10] R.C. Friedman, K.K.H. Farh, C.B. Burge, D.P. Bartel, Most mammalian mRNAs are conserved targets of microRNAs, Genome Res. 19 (1) (2009) 92–105, https://doi.org/10.1101/gr.082701.108.
[11] F. Motta, et al., MicroRNAs in axial spondylarthritis: an overview of the recent progresses in the field with a focus on ankylosing spondylitis and psoriatic arthritis, Curr. Rheumatol. Rep. 23 (8) (Aug. 2021), https://doi.org/10.1007/S11926-021-01027-5.
[12] K. Prajzlerová, et al., Association between circulating miRNAs and spinal involvement in patients with axial spondyloarthritis, PLoS One 12 (9) (Sep. 2017) e0185323, https://doi.org/10.1371/journal.pone.0185323.
[13] B. Meder, et al., Influence of the confounding factors age and sex on microRNA profiles from peripheral blood, Clin. Chem. 60 (9) (2014) 1200–1208, https://doi.org/10.1373/clinchem.2014.224238.
[14] M. Rudwaleit, J. Braun, J. Sieper, ASAS-Klassifikationskriterien für axiale Spondyloarthritis, Z. Rheumatol. 68 (7) (2009) 591–593, https://doi.org/10.1007/s00393-009-0510-y.
[15] S. Ramiro, et al., ASAS-EULAR recommendations for the management of axial spondyloarthritis: 2022 update, Ann. Rheum. Dis. 82 (1) (2022) 10–34, https://doi.org/10.1136/ard-2022-223296.
[16] R. Landewé, A. van Tubergen, Clinical tools to assess and monitor spondyloarthritis, Curr. Rheumatol. Rep. 17 (7) (2015) 1–7, https://doi.org/10.1007/s11926-015-0522-3.
[17] S. Van Der Linden, H.A. Valkenburg, A. Cats, Evaluation of diagnostic criteria for ankylosing spondylitis, Arthritis Rheum. 27 (4) (1984) 361–368, https://doi.org/10.1002/art.1780270401.
[18] T. Hunter, D. Sandoval, N. Booth, E. Holdsworth, A. Deodhar, Comparing symptoms, treatment patterns, and quality of life of ankylosing spondylitis and non-radiographic axial spondyloarthritis patients in the USA: findings from a patient and rheumatologist Survey, Clin. Rheumatol. 40 (8) (2021) 3161–3167, https://doi.org/10.1007/s10067-021-05642-6.
[19] M. Martin, Cutadapt removes adapter sequences from high-throughput sequencing reads, EMBnet.journal 17 (1) (May 2011) 10, https://doi.org/10.14806/ej.17.1.200.
[20] S. Andrews, FastQC: a quality control tool for high throughput sequence data [Online]. Available: https://www.bioinformatics.babraham.ac.uk/projects/fastqc/, 2010.
[21] lh3/seqtk: toolkit for processing sequences in FASTA/Q formats, "lh3/seqtk: toolkit for processing sequences in FASTA/Q formats." [Online]. Available: https://github.com/lh3/seqtk, 2018.
[22] D.M. Vitsios, A.J. Enright, Chimira: analysis of small RNA sequencing data and microRNA modifications, Bioinformatics 31 (20) (2015) 3365–3367, https://doi.org/10.1093/bioinformatics/btv380.
[23] A. Kozomara, S. Griffiths-Jones, MiRBase: annotating high confidence microRNAs using deep sequencing data, Nucleic Acids Res. 42 (D1) (2014) 68–73, https://doi.org/10.1093/nar/gkt1181.
[24] S. Anders, W. Huber, Differential expression analysis for sequence count data, Genome Biol. 11 (10) (2010) R106, https://doi.org/10.1186/gb-2010-11-10-r106.
[25] R Core Team, R: A Language and Environment for Statistical Computing (3.6.3), R Foundation for Statistical Computing, 2020 [Online]. Available: http://www.r-project.org/.
[26] M. Stephens, False discovery rates: a new deal, Biostatistics 18 (2) (2017) 275–294, https://doi.org/10.1093/biostatistics/kxw041.
[27] RStudio Team, RStudio: Integrated Development for R. (1.2.5033), RStudio, Inc., 2019 [Online]. Available: http://www.rstudio.com/.
[28] T. Hothorn, F. Bretz, P. Westfall, Simultaneous inference in general parametric models, Biom. J. 50 (3) (2008) 346–363, https://doi.org/10.1002/bimj.200810425.
[29] H. Wickham, et al., Welcome to the Tidyverse, J. Open Source Softw. 4 (43) (Nov. 2019) 1686, https://doi.org/10.21105/joss.01686.
[30] V. Licursi, F. Conte, G. Fiscon, P. Paci, MIENTURNET: an interactive web tool for microRNA-target enrichment and network-based analysis, BMC Bioinf. 20 (1) (2019) 1–10, https://doi.org/10.1186/s12859-019-3105-x.
[31] X. Baraliakos, J. Braun, Non-radiographic axial spondyloarthritis and ankylosing spondylitis: what are the similarities and differences? RMD Open 1 (Suppl 1) (2015) 8–11, https://doi.org/10.1136/rmdopen-2015-000053.
[32] X. Li, et al., Aberrant expression of microRNAs in peripheral blood mononuclear cells as candidate biomarkers in patients with axial spondyloarthritis, Int. J. Rheum. Dis. 22 (7) (2019) 1188–1195, https://doi.org/10.1111/1756-185X.13563.
[33] M.P. Hunter, et al., Detection of microRNA expression in human peripheral blood microvesicles, PLoS One 3 (11) (2008), https://doi.org/10.1371/journal.pone.0003694.
[34] J. Ma, Y. Lin, M. Zhan, D.L. Mann, S.A. Stass, F. Jiang, Differential miRNA expressions in peripheral blood mononuclear cells for diagnosis of lung cancer, Lab. Invest. 95 (10) (2015) 1197–1206, https://doi.org/10.1038/labinvest.2015.88.
[35] H. Gu, et al., MiR-1-3p regulates the differentiation of mesenchymal stem cells to prevent osteoporosis by targeting secreted frizzled-related protein 1, Bone 137 (2020) 115444, https://doi.org/10.1016/j.bone.2020.115444.
[36] R. Ding, et al., Downregulation of miR-1-3p expression inhibits the hypertrophy and mineralization of chondrocytes in DDH, J. Orthop. Surg. Res. 16 (1) (2021) 1–10, https://doi.org/10.1186/s13018-021-02666-1.
[37] J. Bleil, et al., Cartilage in facet joints of patients with ankylosing spondylitis (AS) shows signs of cartilage degeneration rather than chondrocyte hypertrophy: implications for joint remodeling in AS, Arthritis Res. Ther. 17 (1) (2015) 1–10, https://doi.org/10.1186/s13075-015-0675-5.
[38] L. Zhou, et al., MicroRNA-1-3p enhances osteoblast differentiation of MC3T3-E1 cells by interacting with hypoxia-inducible factor 1 α inhibitor (HIF1AN), Mech. Dev. 162 (February) (2020) 103613, https://doi.org/10.1016/j.mod.2020.103613.
[39] P. Miossec, Local and systemic effects of IL-17 in joint inflammation : a historical perspective from discovery to targeting, Cell. Mol. Immunol. (March) (2021), https://doi.org/10.1038/s41423-021-00644-5.
[40] S.I. Jang, M. Tandon, L. Teos, C.Y. Zheng, B.M. Warner, I. Alevizos, Dual function of miR-1248 links interferon induction and calcium signaling defects in Sjögren's syndrome, EBioMedicine 48 (2019) 526–538, https://doi.org/10.1016/j.ebiom.2019.09.010.
[41] Y.P. Tang, et al., Circular RNAs in peripheral blood mononuclear cells from ankylosing spondylitis, Chin. Med. J. 134 (21) (2021) 2573–2582, https://doi.org/10.1097/CM9.0000000000001815.

[42] P. Ruiz-Limon, et al., Potential role and impact of peripheral blood mononuclear cells in radiographic axial spondyloarthritis-associated endothelial dysfunction, Diagnostics 11 (6) (2021) 1–17, https://doi.org/10.3390/diagnostics11061037.
[43] N. Rosine, C. Miceli-Richard, Innate cells: the alternative source of IL-17 in axial and peripheral spondyloarthritis? Front. Immunol. 11 (January) (2021) 1–12, https://doi.org/10.3389/fimmu.2020.553742.
[44] K. Pawlina, T. Tomasz, Benchmarking of bioinformatics tools for NGS - based microRNA profiling with RT - qPCR method, Funct. Integr. Genomics 23 (4) (2023) 1–11, https://doi.org/10.1007/s10142-023-01276-w.
[45] J. Pepe, et al., Characterization of extracellular vesicles in osteoporotic patients compared to osteopenic and healthy controls, J. Bone Miner. Res. 00 (00) (2022) 1–15, https://doi.org/10.1002/jbmr.4688.
[46] M.C.X. Pinto, et al., Calcium signaling and cell proliferation, Cell. Signal. 27 (11) (2015) 2139–2149, https://doi.org/10.1016/j.cellsig.2015.08.006.
[47] K. Qi, et al., Long non-coding RNA (lncRNA) CaIF is downregulated in osteoarthritis and inhibits LPS-induced interleukin 6 (IL-6) upregulation by downregulation of miR-1246, Med. Sci. Monit. 25 (2019) 8019–8024, https://doi.org/10.12659/MSM.917135.
[48] G.W. Krissansen, et al., Overexpression of miR-595 and miR-1246 in the sera of patients with active forms of inflammatory bowel disease, Inflamm. Bowel Dis. 21 (3) (2015) 520–530, https://doi.org/10.1097/MIB.0000000000000285.
[49] M. Husakova, Micrornas in the key events of systemic lupus erythematosus pathogenesis, Biomed. Pap. 160 (3) (2016) 327–342, https://doi.org/10.5507/bp.2016.004.
[50] W.P. Maksymowych, Biomarkers for diagnosis of axial spondyloarthritis, disease activity, prognosis, and prediction of response to therapy, Front. Immunol. 10 (MAR) (2019) 1–9, https://doi.org/10.3389/fimmu.2019.00305.
[51] D.E. Furst, J.S. Louie, Targeting inflammatory pathways in axial spondyloarthritis, Arthritis Res. Ther. 21 (1) (2019) 1–15, https://doi.org/10.1186/s13075-019-1885-z.
[52] M. Silacci, et al., Discovery and characterization of COVA322, a clinical-stage bispecific TNF/IL-17A inhibitor for the treatment of inflammatory diseases, mAbs 8 (1) (2016) 141–149, https://doi.org/10.1080/19420862.2015.1093266.
[53] T. Andersen, et al., Increased plasma levels of IL-21 and IL-23 in spondyloarthritis are not associated with clinical and MRI findings, Rheumatol. Int. 32 (2) (2012) 387–393, https://doi.org/10.1007/s00296-010-1655-3.